Contrastive analysis of dynamic response of tailings dam with and without geofabriform by shaking table model test

Qiaoyan Li[1,2,*] , Guowei Ma[1,3], Ping Li[2], and Zhandong Su[2]

[1]College of Architecture and Civil Engineering, Beijing University of Technology, Beijing, 100124,China
[2]Institute of Disaster Prevention, Hebei, 065201, China
[3]School of Civil and Transportation Engineering, Hebei University of Technology, Tianjin, 300401, China

Abstract. Construction using geofabriform is a new promising technology to build fine grain tailings dam. Large-scale shaking table tests are conducted in this study to investigate the dynamic performances in terms of horizontal acceleration and displacement of the tailings dam with and without geofabriform subject to horizontal earthquakes. Test results indicate that the seismic performance of the tailings dam with geofabriform is significantly better than that of tailings dam without geofabriform. The two types of tailings dams have different failure modes under the action of earthquake. The acceleration amplification factor(A_m), vertical displacement and horizontal displacement of the tailings dam with geofabriform under the same seismic acceleration input are smaller than that of the tailings dam without geofabriform, the maximum attenuation amplitude of the A_m at the dam slope reaches to 81%. The horizontal displacements of the two types of dams are nonlinearly distributed in the height direction and the geotextile bags of the tailings dam have an upward displacement and are tilted upward. According to the failure mode of the tailings dam with geotextile bags, it is recommended to strengthen the drainage measures and set up anti-slide piles at the bottom of the geotextile bags body to strengthen the tailings dam.

1 Introduction

With the continuous improvement of the beneficiation technology and recovery rate, tailings have less coarse particles larger than 0.074mm and more fine particles less than 0.03mm. Fine-grained tailings are characterized by poor water permeability after storage, long consolidation time, low mechanical strength, and difficulty in dissipating excess pore water pressure. The upstream method of dam construction is simple and easy to manage, and has been widely used in China for decades. But it requires large amounts of coarse particles to construct tailings embankment. If the traditional upstream storage method is used for fine-grained tailings, problems such as difficulty in dam construction, poor drainage of the dam body, slow slope of the sedimentary beach, and poor stability are often encountered. The fine tailings dams constructed by an upstream method may have many issues, such as difficulties in dam construction, low permeability, the slow consolidation of tailings and poor stability of the dam.

Therefore, how to improve the stability of tailings dam is a challenge for mine operators and it is of great significance to study the stability of fine tailings dam. Utilizing geotextile tubes for tailings dam construction is a remedy for all these problems.

As well known, the geofabriform method employs a geotextile bag filled with natural soil material, tailings, and other bulk materials to constitute the geotechnical composite soil with specific strength by drainage and consolidation[1]. This method was first applied in Netherlands to build the delta project[2].The project of increasing breakwater of Mississippi River was carried out using the geofabriform method[3]. In light of the successes of these two projects, the geofabriform method has been increasingly applied by the researchers from over 32 countries in Asia, Europe, and the Americas. The application includes the slope protection projects of seawall and coast, ports, tunnels, channels, flood dikes, railways, highways, etc.[4-10]. The geofabriform method was initially applied in the field of mining to overcome the obstacles in building the fine-grain tailings dam in China[1]. Fig.1 is a close-in partial view of a practical tailings dam using geofabriform method in Yunnan province of China. Fig.2 is a schematic of cross-section of a tailings dam using geofabriform method.

(a) Inside of tailings dam   (b) Outside of tailings dam
Fig.1 Close-in partial view of tailings dam using geofabriform method in Yunnan province
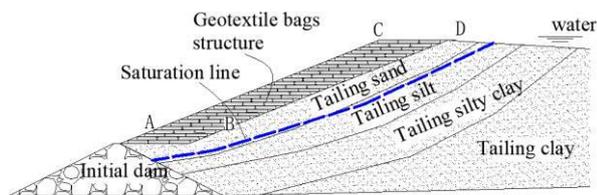
---

* Qiaoyan Li: liqiaoyan@cidp.edu.cn

Fig.2 Schematic of cross-section of tailings dam using geofabriform method

At present, the research on the geofabriform method mainly focuses on the study of the mechanical properties of the geotextile bags[11-15] and the stability of the geotextile bags subject to sea wave[16-19]. Some other studies were conducted on the mechanical properties, stability, and engineering applications of tailings dam using geofabriform method[20-23]. In addition, there are very limited studies on the dynamic response and stability of the tailing dam using geofabriform method subject to earthquake. Understanding the seismic performance of the tailings dam with geofabriform method is critical for appropriate design in a country like China that is prone to earthquakes. To promote the general application of the geofabriform method for tailings dam in the field of mining, it is imperative to conduct in-depth research to exposit the aforementioned issues.

In this paper, the contrastive analysis of the dynamic response of the tailings dam with and without geofabriform under different horizontal earthquakes is investigated by large-scale shaking table model test. It aims to provide theoretical support for promotion of application of the tailings dam based on geofabriform method.

2 Test overview

2.1 Test system and equipment

The test is conducted at the Civil Engineering Test Center of the Institute of Disaster Prevention of China Earthquake Administration. The shaking table is an electro-hydraulic servo two-way shaking table with dimensions of 3.0m×3.0m, maximum load capacity of 20 tons, operating frequency range of 0.4-80Hz, maximum overturning moment of 400kN•m, and maximum displacement of ±20cm. The maximum speed is 80cm/s, and the maximum horizontal acceleration of the table is 2.0g at full load. A 128-channel dynamic acquisition system is used for data acquisition.

2.2 Model design

Considering the size and maximum load of the shaking table, the size of the test model box is designed to be 2.7m × 1.0m × 1.0m. The two long sides (Side A and Side B) of the model box are made from plexiglass for clear observation, and a short end is left open to input load. The bottom edge of the model box and the other short side are made from steel plates. The model box is reinforced with 120 channel steel connecting side A and

B of the box for rigorous integrity. It is fixed on the shaking table by 6 bolts.

The geotextile bag structure is 40cm wide and 80cm high with a slope ratio of 1:1, consisting of 16 layers of 20cm×20cm×5cm geotextile bags filled with fine tailings.

The test materials are the same geotextile and tailings as those at the construction site of a practical tailings dam in Yunnan Province. The physical parameters of the tailings, the particle composition, and the basic mechanical parameters of the geotextile are shown in Tables 1-3[21].

Table1. Physical parameters of tailings

Unit weight /(kN/m³)	Void ratio e	Compression modulus E_s/ Mpa	Compression factor a/Mpa^{-1}	Consolidated quick shear strength	
				c/kpa	/(°)
20	0.63	73.29	0.15	16	21

Table2. Actual size composition of tailings

Particle size range / mm	≤0.019	≤0.037	≤0.05	≤0.074
Mass percentage /%	56.64	68.44	73.29	79.89

Table3. Basic mechanical parameters of the geotextile

| Test projects			unit	average value	Reference standard
Mechanica properties	Mass per unit area		g/m²	151	GB/T13762-2009
	Thickness (2kPa)		mm	0.62	GB/T13761.1-2009
	Breaking strength	T	N/5cm	1520	GB/T 3923.1-2013
		W		1210	GB/T 3923.1-2013
	Elongation at break	T	%	20.3	GB/T 3923.1-2013
		W		18.7	GB/T 3923.1-2013

In this test, a total of eight pore pressure sensors (K1~K8) are installed at two different positions in each layer with a total four layers along the height of the tailings dam. There are eighteen accelerometers, including twelve 941B accelerometers, placed in the tailings as denoted by J1~J12.They are deployed at two different positions in each layer with a total six layers along the depth. Four piezoelectric sensors are positioned on each side of the geotextile bags structure, which are indicated by JY1~JY4. Other two 941B accelerometers are placed on each of the two sides along the input acceleration direction of the shaking table to measure the practical triggering acceleration of the shaking table. Five ejector pins displacement meters are deployed on one side of the geotextile bag structure, which are denoted byW1~W5. W1~W5 are placed at elevations of 25cm, 40cm, 55cm, 70cm, and 75cm, respectively. The sensor layout is shown in Fig. 3.

(a) The model of the tailings dam with geofabriform
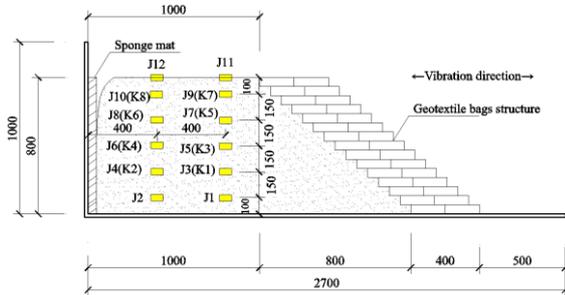
(b) Schematic of the longitudinal profile of the model
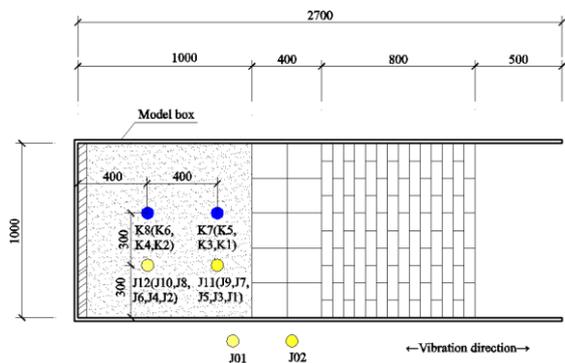
(c) Top view of the model

Fig. 3 Part of sensor layout of the shaking table test for tailings dam with geofabriform

2.3 Loading scheme

The horizontal seismic wave is representative earthquake load. Thus, the input seismic wave of this test is a one-way horizontal WoLong wave. A typical applied seismic time-history curve is shown in Fig. 4.
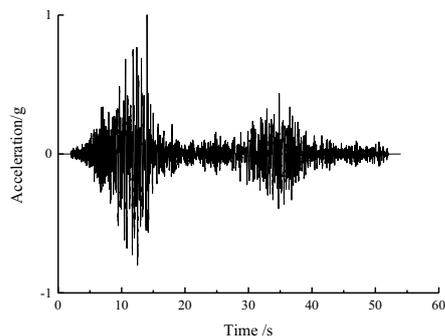

Fig. 4 Seismic time-history wave

To identify the specific wave intensity to incur dynamic damage to the tailings dam, the test is conducted with increasing respective gravitational accelerations of 0.1g, 0.2g, 0.6g, 0.8g, 1.0g, 1.2g, 1.6g, g, respectively. Due to the limitation of the precision of the hydraulic jack, the peak accelerations of the actual output of the shaking table are 0.1g, 0.3g, 0.6g, 0.7g, 0.9g, 1.0g, and 1.3g, respectively. The acceleration of the shaking table acts as the horizontal seismic ground acceleration loads. Failure status of the dam is evaluated by the ratio of the maximum horizontal displacement D_{max} to the total height of the dam H_t, i.e., D_{max}/H_t. If the ratio exceeds 0.1, the dam is considered to be failed[24,25].
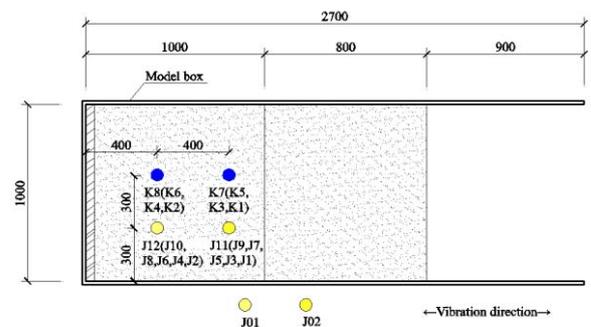
For comparison, the shaking table test of the tailings dam without geofabriform under the same conditions is also carried out. The model and sensor layout are shown in Fig.5.
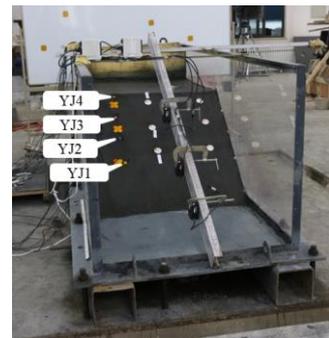
(a) The model of the tailings dam without geofabriform
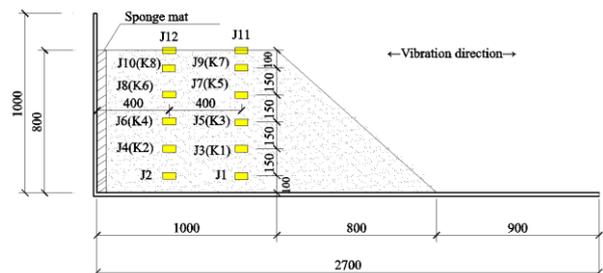
(b) Schematic of the longitudinal profile of the model without geofabriform

(c) Top view of the model without geofabriform
Fig.5 Part of the sensor layout of the shaking table test for tailings dam without geofabriform

3 Failure mode analysis

The two tailings dams have different failure modes. Both the upper part of the two tailings dams where the maximum shear stress occurs vibrate strongly. For the

tailings dam without geofabriform, the cracks are observed on the dam crest and slope plane, running through to form a slip surface under the action of maximum shear stress. When the dam fails, the part above the slid plane of the dam is dumped downwards, and then the whole dam body slides forward, resulting in a dam collapse, as shown in Fig.6. However, for the tailings dam with geofabriform, due to the supporting effect of the geofabriform on the slope surface, there are only cracks observed on the top of the dam. The geofabriform effectively prevents the cracks from expanding, running through and the formation of the sliding plane. When the dam fails, the whole dam slid forward without collapse, as shown in Fig.7. The geofabriform increases the stability of the dam.

Fig.6 Failure of the tailings dam without geofabriform

Fig.7 Failure of the tailings dam with geofabriform

4 Test results analysis

4.1 Acceleration amplification factor A_m

The acceleration amplification factor A_m is defined as the ratio of the maximum acceleration of each measurement point to the input peak vibration acceleration of the shaking table surface. Fig.8 shows the A_m at JY1, JY2, JY3, and JY4 on the slope of the two types of dams when HPGA is 0.3g, 0.6g, 0.9g, and 1.0g. It shows that the A_m of the tailings dam with geofabriform is significantly lower than that of the tailings dam without geofabriform. The maximum reductions can reach 56%, 71%, 73%, and 81%, respectively. Because the geofabriform itself has flexibility and can be deformed by itself, also the tailing slurry formed by the liquefaction of the tailings in the tailings reservoir area buffers the earthquake effect, resulting in a decrease of A_m, which indicates that the geofabriform has good shock absorption performance.

Fig.9 shows the amplification factor A_m against HPGA on the slope of the two types of tailings dam. It shows that the A_m has an alternative decrease-increase-

decrease with the increase of HPGA. For the tailings dam without geofabriform, when HPGA < 1.0g, the A_m at each measurement point on the dam is not much different under the same HPGA. That is because the dam is a whole with. When HPGA≥1.0g, the difference of A_m at each measurement point becomes larger, especially the A_m of JY3 increases more, because the elevation of JY3 is 55cm, which is located in the middle and upper part of the dam, where the vibration is stronger. this is consistent with the greater vibration of the upper part of the dam in the experimental phenomenon.

The JY1, JY2 and JY4 of the tailings dam with geofabriform have a little variation with the increase of HPGA. Similarly, JY3 changes greatly. When HPGA is 0.9g, the geofabriform body reached the ultimate failure state, and A_m of JY3 reached the maximum value, and then the geofabriform layers start sliding off each other which caused the failure and the reducing of A_m.
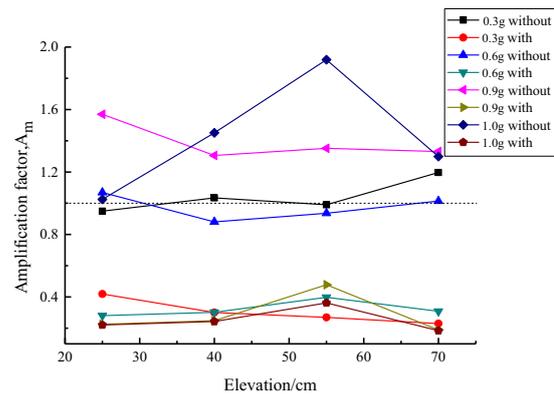

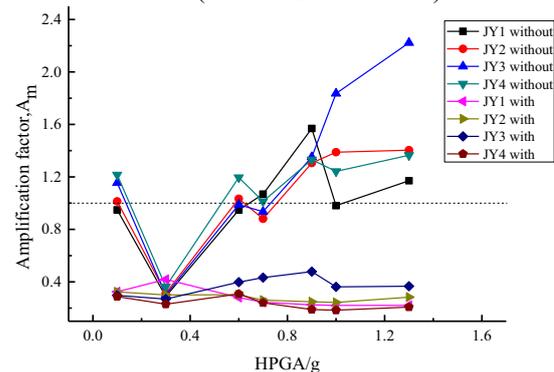**Fig.8** Amplification factor A_m against elevation at different HPGA (YJ1、YJ2、YJ3、YJ4)

Fig. 9 Amplification factor A_m against HPGA of the two tailings dam (YJ1, YJ2, YJ3, YJ4)

Fig.10 shows the A_m of the dam crest at different HPGA. For J11 and J12 at the top of the tailings, when the HPGA is small, the A_m of the tailings dam with geofabriform is slightly larger than the tailings dam without geofabriform. With the increase of HPGA, the A_m of the tailings dam with geofabriform is reduced, while the A_m of the tailings dam without geofabriform is gradually increased. For the final failure, the A_m of the tailings dam without geofabriform is much larger than the tailings dam with geofabriform. For JY4 on the slope of the dam, the A_m of the tailings dam without geofabriform is much larger than that of the tailings dam with geofabriform. The A_m of the tailings dam without

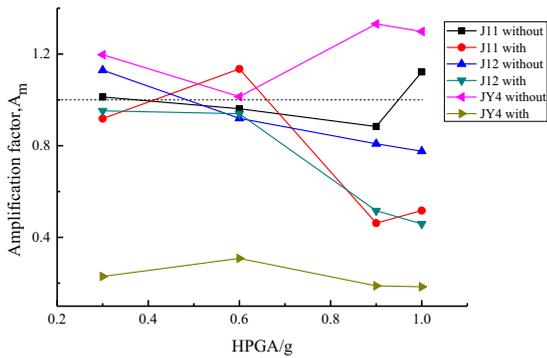geofabriform all is greater than 1, while the A_m of the tailings dam with geofabriform is less than 1.

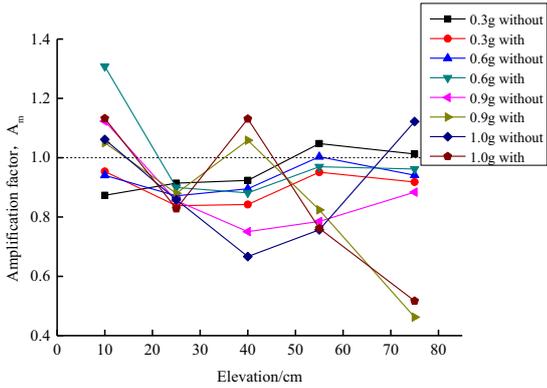**Fig.10** Amplification factor A_m at the dam crest against HPGA

Fig.11 Amplification factor A_m against elevation at different HPGA (J1, J3, J5, J7, J11)

Fig.11 is the A_m of J1, J3, J5, J7, and J11 which are at the same location from top view but different vertical elevations when HPGA is 0.3g, 0.6g, 0.9g, and 1.0g. It shows that when the HPGA is small, the A_m of the two tailings dams is not much different. With the increase of HPGA, the A_m in the middle height of the tailings dam with geofabriform is significantly larger than that of the tailings dam without geofabriform. For the final failure, the A_m of the tailings dam without geofabriform is much larger than that of the tailings dam with geofabriform.

4.2 Vertical displacement

Fig.12 shows the relationship between the vertical displacement of the marked point of the side A on the dam slope and the elevation when the HPGA is 0.3g, 0.6g, 0.9g, and 1.0g. It shows that under the same HPGA, the vertical displacement of the tailings dam without geofabriform is greater than that of the tailings dam with geofabriform. For the tailings dam without geofabriform, the vertical displacement increases with the increase of the elevation and HPGA. For the tailings dam with geofabriform, the vertical displacement increases with the increase of the elevation, but with the increase of HPGA, some marked point at the bottom of the geofabriform structure shows a negative vertical displacement, indicating that the outer side of the geofabriform body has an upward displacement. The geofabriform body is tilted up, which is consistent with the experimental imagination.
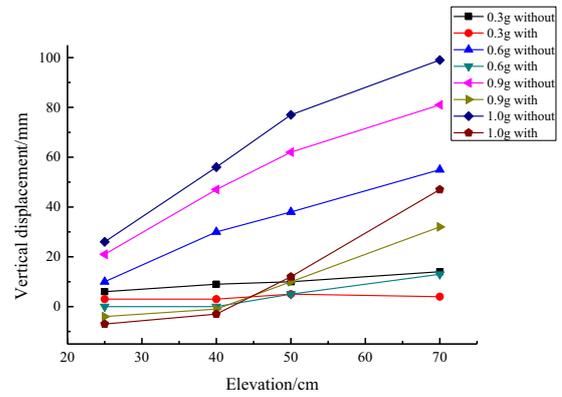

Fig.12 Comparison of the vertical displacement of the side A of the two tailings dams
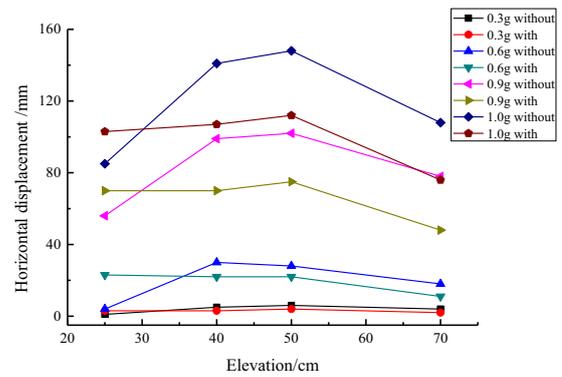

Fig.13 Comparison of the horizontal displacement of the side A of the two tailings dams

4.3 Horizontal displacement

Fig.13 shows the relationship between the horizontal displacement of the marked point of the side A on the dam slope and the elevation when the HPGA is 0.3g, 0.6g, 0.9g, and 1.0g. It shows that under the same HPGA, the maximum horizontal displacement of the tailings dam without geofabriform is greater than that of the tailings dam with geofabriform. The horizontal displacements of the two tailings dams show a nonlinear distribution with the increase of height, which are small at the bottom and the top of the dam, while have the maximum in the middle, coinciding with the outward protrusion of the dam body in the experimental phenomenon. When HPGA=0.9g, the maximum horizontal displacement of the tailings dam without geofabriform reached 102mm, 102mm/800mm=12%>10%, the dam failed. When HPGA=1.0g, the maximum horizontal displacement of the tailings dam with geofabriform reached 112mm, 112mm/800mm=14%>10%, the dam failed.

4.4 Analysis of test results

The test results show that the seismic performance of the tailings dam with geofabriform is better than that of the tailings dam without geofabriform subject to different input acceleration for the same size tailings dam. Therefore, the tailings dam with geofabriform is a flexible structure with low deformation modulus, strong

tensile strength, high damping, and good deformation ability and ability to consume seismic energy subject to strong earthquakes. When it fails, the entire dam slides forward. It doesn't like the tailings dam without geofabriform to collapse but still maintains overall stability and has good seismic performance.

According to the failure mode of the tailings dam with geotextile bags, it is recommended to strengthen the drainage measures and set up anti-slide piles at the bottom of the geotextile bags body to strengthen the tailings dam

5 Conclusion

Through large-scale shaking table test, the acceleration and displacement of the monitoring points also the failure mode of the tailings dam with and without geofabriform subject to different input seismic accelerations are compared and analyzed. Based on the indoor test results, the seismic strengthening measures of the tailings dam with geofabriform are proposed. The following conclusions are derived:

(1) Two tailings dams have different failure modes under earthquake action. With the increase of the input seismic acceleration, the upper part of the dam body whose range is about 1/3 height of the dam vibrates greatly for the two tailings dams. The part of the dam body with large vibration is dumped downwards, resulting in a dam collapse for tailings dam without geofabriform. In the case of the tailings dam with geofabriform, the whole dam slides forward without collapse.

(2) Under the same seismic acceleration input, the acceleration amplification factor, vertical displacement and horizontal displacement of the tailings dam with geofabriform are less than that of the tailings dam without geofabriform.

(3) It is recommended to strengthen the drainage facility and set up anti-slide piles at the bottom of the geotextile bags body to reinforce the tailings dam with geofabriform to improve its stability.

Acknowledgements

References

1. H.M. Zhou , Nonferrous Metals (Mining Section), **63(5)**,1-3(2011)
2. H. Perrier, Proceedings of 3rd International Conference on Geotextiles,Vienna , Austria , 1115 – 1119(1986)
3. J. Fowler, Geotechnical Fabrics Report, **15 (5)**, 28 – 37 (1997)
4. C.R. Lawson, Geosynthetics International, **15(6)**, 384-427(2008)
5. K. Spelt, Terra et Aqea, **83**, 21-25(2011)
6. G.R. Koerner, R.M. Koerner, Geotextiles and Geomembranes, **24**,129-137(2006)
7. R.M. Koerner, G.R. Koemer, Geotechnical Testing Journal, **33(3)**, 1-7(2010)
8. Y.I. Oh, E.C. Shin, Coastal Engineering, **53(11)**, 879-895(2006)
9. E.C. Shin, Y.I. Oh, Geotextiles and Geomembranes **25(4-5)**, 264-277(2007)
10. S.J. Restalla, L.A. Jacksonb, G. Heertenc, et al., Geotextiles and Geomembranes, **20(5)**, 214-342(2002)
11. V. Namias, Journal of applied mechanics, **52**,913-918(1985)
12. D. Leshchinsky, O. Lesbchinsky, H. I.Ling, et al., Journal of Geotechnical Engineering, **122(8)**,682-690(1996)
13. C.L. Qiu, Y. Yan, S.W. Yan, Chinese Journal of Geotechnical Engineering, **30(5)**, 760-763(2008)
14. R.H. Plaut, S.A .Cotton, Journal of Sound and Vibration, **282**,265-276(2005)
15. S.H. Liu, H. Matsuoka, Rock and Soil Mechanics **28(8)**,1665-1670(2007)
16. R.H. Plaut, C.R. Klusman, Thin-Walled Structures, **(34)**,179-194(1999)
17. S.Cantré, Geotextiles and Geomembranes, **20(5)**, 305-319(2002)
18. F. Saathoff, H. Oumeraci, S. Restall, Geotextiles and Geomembranes, **25(4-5)**, 251-263(2007)
19. H. Matsuoka, Japanese Society of Tribologists, **48(7)**, 547-52 (2003)
20. H.M. Zhou, *Techonology of tailings damming with geofabriform method.* (Beijing: Metallurgical Industry Press,2015)
21. Q.Y. Li, H.D. Wang, G.W. Ma, et al., Rock and Soil Mechamics, **37(4)**,957-964(2016)
22. X. Cui, H.M. Zhou, Y.B. Qie, et al., Nonferrous Metals Mieral Processing Section **(1)**, 60-64(2016).
23. X.F. Liu, J. Guo, Nonferrous Metals(Mine Section) **68(5)**, 82-86(2016)
24. C.C. Huang, H.J. Wu, Geosynthetics International **16(3)**, 222–234(2009)
25. Y.Wu, S. Prakash, ASCE Geotechnical Special Publication: Analysis and Design of Retaining Structures Against Earthquakes, S. Prakash, Editor, ASCE, New York, 21–37(1996)